Chemical Physics Letters 463 (2008) 1–10

Contents lists available at ScienceDirect

Chemical Physics Letters

journal homepage: www.elsevier.com/locate/cplett

FRONTIERS ARTICLE

The hydrogen bond

A.D. Buckingham [a,*], J.E. Del Bene [b], S.A.C. McDowell [a,1]

[a] Department of Chemistry, Cambridge University, Cambridge CB2 1EW, UK
[b] Department of Chemistry, Youngstown State University, Youngstown, OH 44555, USA

ARTICLE INFO

Article history:
Received 30 May 2008
In final form 9 June 2008
Available online 24 June 2008

ABSTRACT

The concept of the hydrogen bond is a century old but remains youthful because of its vital role in so many branches of science and because of continued advances in experiment, theory and simulation. We discuss the structural and energetic characteristics of normal hydrogen bonds X–H···Y as well as some exceptions to the normal, including proton-shared and ion-pair bonds. We consider the harmonic and anharmonic vibration of X–H in a variety of complexes, and demonstrate that there is no fundamental difference between blue-shifting and red-shifting bonds. We discuss water clusters and liquid water and indicate possible directions of future progress.

1. Introduction

A hydrogen bond is an attraction between a proton donor X–H and a proton acceptor Y. In a *normal* hydrogen bond, as in the water dimer, there is a strong directional attraction of the X–H bond to an electron-rich region on the proton acceptor Y. The strength of this bond as measured by the binding energy D_e can be up to about 30 kJ mol^{-1}, but binding energies vary over a wide range. The linear symmetrical bifluoride anion $[F–H–F]^-$ has a dissociation energy D_0 to HF + F^- of 167 kJ mol^{-1} and should be considered as a chemically bound species rather than as an HF molecule interacting with F^-. An H–Cl molecule and a Ne atom are bound by 1.6 kJ mol^{-1} in the Cl–H···Ne van der Waals molecule but the H–Cl enjoys nearly free rotation within the complex, so is the binding due to a hydrogen bond? The literature abounds with mystical statements about the hydrogen bond. For example, a well known textbook states: 'Because the bonding depends on orbital overlap, the H-bond is virtually a contact-like interaction that is turned on when XH touches Y and is zero as soon as the contact is broken' [1].

IUPAC has recently had a panel of experts considering the nature of the hydrogen bond. They propose the following tentative definition [2]: 'The hydrogen bond is an attractive interaction between a group X–H and an atom or group of atoms Y in the same or different molecule(s), where there is evidence of bond formation'.

The history of the concept is well described by Smith [3] and Hadži [4]. It is approximately 100 years old but remains youthful because of continuing advances in experimental, theoretical and simulation techniques. Many books have been devoted to the hydrogen bond. Pimentel and McClellan's *The Hydrogen Bond* [5] has been influential for nearly 50 years, and in recent years there have appeared: *Theoretical Treatments of Hydrogen Bonding* [6], *Hydrogen Bonding. A Theoretical Perspective* [7], *An Introduction to Hydrogen Bonding* [8] and *The Weak Hydrogen Bond* [9]. The debate about the origin of hydrogen bonding (see, for example, Coulson's short review [10]) has largely been relegated to history because the quantum-mechanical nature of chemical bonding is now universally accepted. The wide range of hydrogen-bond energies means that the different types of interaction energies, i.e. electrostatic, induction, electron delocalisation, exchange repulsion and dispersion, make different relative contributions to the overall energy of the hydrogen bond. However, for the vast majority of *normal* hydrogen bonds in the vapor and condensed phases, the electrostatic-plus-induction description provides a near-quantitative account of the attractive force responsible for the interaction, and has the virtue of simplicity. The strength of a normal hydrogen bond in relation to the thermal energy kT at room temperature ($kT \sim 2.5$ kJ mol^{-1}) means that it is of prime importance in biology.

In this Letter we discuss the characteristics of normal hydrogen bonds, as well as some of the exceptions to the normal, such as *proton-shared* and *blue-shifting* hydrogen bonds. In the case of the $BrH\cdots NH_3$ complex, application of a modest electric field in the direction of the hydrogen bond from Br to N changes the normal bond into a proton-shared bond and finally to the ion pair $Br^- \cdots NH_4^+$; such a change provides insight into how solvent effects can dramatically change the properties of a solute. We include sections on the structures and vibrational frequencies of hydrogen-bonded complexes, and on the important case of hydrogen bonding in water. Recent spectroscopic investigations of water clusters and particularly the dimer, combined with theoretical advances in evaluating intermolecular forces, have led to greatly improved accuracy in our description of the potential energy surface

* Corresponding author.
E-mail address: abd1000@cam.ac.uk (A.D. Buckingham).
[1] Permanent address: Department of Biological and Chemical Sciences, University of the West Indies, Cave Hill Campus, Bridgetown, Barbados.

0009-2614/$ - see front matter © 2008 Elsevier B.V. All rights reserved.
doi:10.1016/j.cplett.2008.06.060

of the water dimer. If the parameterised representation of this surface includes induction, then it can be used successfully for larger clusters and for the condensed phases. As a result, our understanding of liquid water is moving from an art form towards a quantitative science.

2. Structures of hydrogen-bonded complexes

Although a normal X–H···Y hydrogen bond is weak relative to covalent bonds, it is usually strong enough to hold two molecules together so that they have a definite structure in the ground state of the complex, although there are usually large-amplitude anharmonic zero-point fluctuations about the equilibrium structure. The resulting hydrogen-bonded complex has three significant structural features: the intermolecular X–Y distance, the approximate linearity of the hydrogen bond, and the orientation of the proton-acceptor molecule containing Y. Experimental characterization of these structural features first came from gas-phase microwave spectroscopic studies of the prototypical hydrogen-bonded complexes $(HF)_2$ [11] and $(H_2O)_2$ [12]. The equilibrium structure of $(HF)_2$ was described as having an F–F distance of 2.79 Å, a linear F–H···F hydrogen bond, and an angle of about 108° between the F–F line and the proton-acceptor F–H bond. The water dimer has a *trans* structure, meaning that the non-hydrogen-bonded O–H bond of the proton-donor molecule is *trans* to the bisector of the H–O–H angle of the proton acceptor, as illustrated in Scheme 1. This complex has an intermolecular O–O distance of 2.98 ± 0.04 Å, a nearly linear O–H···O hydrogen bond, and an angle of 120 ± 10° between the O–O line and the bisector of the acceptor H–O–H angle. These features of the water dimer have been reproduced by *ab initio* calculations [13].

The H atom of the proton donor seeks to bind to a region of high electron density on the proton acceptor, often at a lone pair of electrons. Thus, in the water dimer an O–H bond in the proton donor is directed to a lone pair on the O atom of the proton-acceptor molecule. Hydrogen-bond formation and protonation occur in this same lone-pair direction on the proton acceptor. Protonation of H_2O leads to a C_{3v} structure for H_3O^+, and of HF to a bent structure for FH_2^+, but these ions are covalently bound with identical O–H and F–H bonds. The structures of these protonated ions are in contrast to the structures found for complexes in which a simple cation like Li^+ interacts with these bases, since the cation sits at the negative end of the dipole moment vectors of H_2O and FH so as to enhance the electrostatic interaction energy.

Why is a *trans* arrangement preferred in $(H_2O)_2$, since rotation by 180° of the proton-acceptor molecule about the hydrogen-bonding O–O axis preserves both the linearity of the hydrogen bond and the directionality of the lone pair? It is here that secondary factors must be taken into account. These include the relative orientation of the dipole moment vectors of the proton donor and acceptor molecules, and long-range interactions involving atoms or groups of atoms bonded to X and Y. Thus, the *trans* arrangement of $(H_2O)_2$ is preferred to the *cis*, which has an unfavorable alignment of molecular dipole moment vectors. Long-range interactions and short-range packing requirements in the case of crystals can significantly change the structure of a hydrogen bond by distorting it from linearity or changing the orientation of the lone pair relative to the proton donor X–H group. At short range the orientation-dependence of the intermolecular potential energy surface is dominated by the exchange-repulsion forces.

Distorted hydrogen bonds are found in cyclic complexes which are stabilized by two hydrogen bonds. An interesting example is found for the $FH{:}CCl_3H$ system [14,15] which has two minima on the potential surface. One has an open structure with a typical linear F–H···Cl hydrogen bond. The other is cyclic and stabilized by two distorted hydrogen bonds, as shown in Scheme 2. The computed binding energies of the open and cyclic forms are 10.5 and 12.5 kJ mol^{-1}, respectively.

Complexes with distorted hydrogen bonds may also form when one molecule bridges two hydrogen-bonding sites in another molecule. A typical example of this type of hydrogen bond is found in the H_2O:pyridone complex [16–18] with H_2O acting as a proton acceptor for a distorted N–H···O hydrogen bond, and a proton donor for an O–H···O hydrogen bond, as illustrated in Scheme 3. That the presence of a lone pair of electrons on the proton acceptor is a factor in hydrogen-bond formation can be inferred by the rotation of the non-hydrogen-bonded O–H of H_2O out of the hydrogen-bonding plane. This allows one of the oxygen lone pairs to lie approximately in this plane, which strengthens the N–H···O bond.

Another structural motif for a hydrogen-bonded complex is one in which the hydrogen bond is 'bifurcated', as shown in Scheme 4

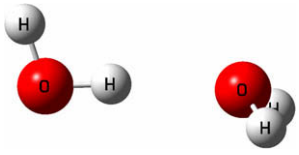

Scheme 1. The water dimer.

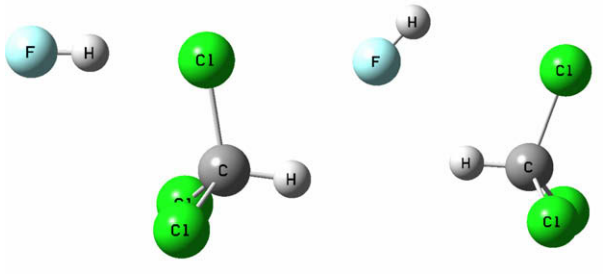

Scheme 2. Equilibrium open and cyclic structures of $FH{:}CCl_3H$.

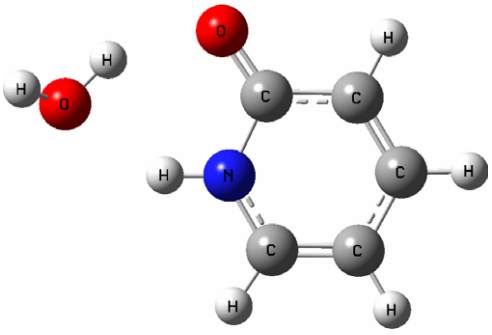

Scheme 3. A bridging H_2O hydrogen-bonded to pyridone.

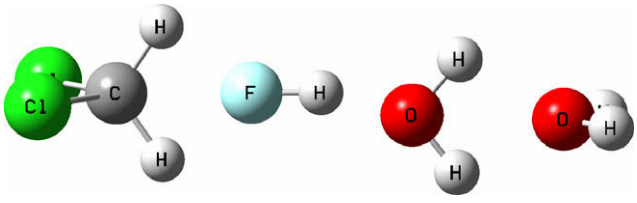

Scheme 4. The structures of the $CCl_2H_2{:}FH$ complex and the water dimer with bifurcated hydrogen bonds.

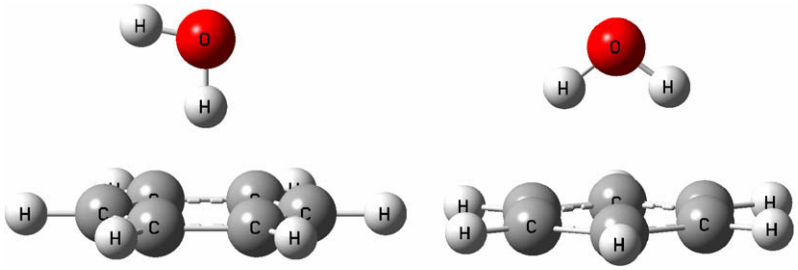

Scheme 5. The hydrogen-bonded $H_2O{:}C_6H_6$ with H_2O in two different orientations.

for the CCl_2H_2:FH complex [15] and for the bifurcated water dimer which is a transition structure on the dimer potential surface for the interchange of the two H atoms of the proton-donor molecule [19]. In structures of this type, one molecule is a double proton donor and the other a double proton acceptor. The hydrogen bonds are nonlinear and relatively weak.

Since hydrogen-bond formation tends to occur at a region of high electron density on the proton-acceptor molecule, it is possible for a hydrogen bond to form through the π-electron system of a molecule. The existence of such π-complexes has been documented experimentally for the H_2O:benzene complex [20,21] illustrated in Scheme 5. The H_2O molecule is located near the C_6 rotational axis of benzene and has little or no barrier to internal rotation. It is also possible for simple unsaturated hydrocarbons to form π hydrogen bonds, as illustrated for the FH:HCCH system in Scheme 6. Two equilibrium complexes exist on the potential surface, one with FH as the proton donor to HCCH through the π cloud, and the other with HCCH as the proton donor to FH through the fluorine lone pairs. The binding energies of the π and lone-pair complexes are 18.9 and 8.2 kJ mol,$^{-1}$, respectively.

All of the hydrogen-bonded complexes discussed thus far contain two neutral molecules. If the proton donor is a cation, then the electrostatic component of the stabilization energy assumes increased importance and may alter the structure of the hydrogen bond. A typical example is the complex illustrated in Scheme 7 in which NH_4^+ acts as a proton donor to H_2O. In this complex the hydrogen bond is linear and the proton-acceptor water molecule is oriented to give the most favorable charge–dipole moment interaction.

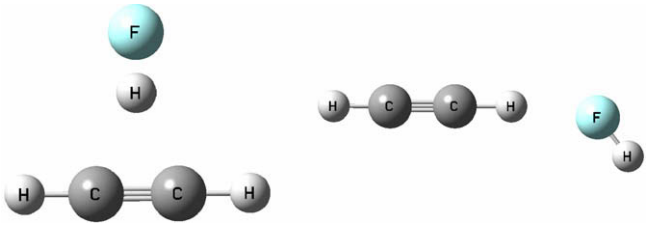

Scheme 6. Two equilibrium FH:HCCH complexes.

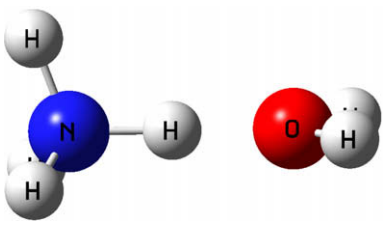

Scheme 7. The NH_4^+:OH_2 complex.

Most hydrogen-bonded complexes formed from two neutral molecules are stabilized by *normal* (also called *traditional*) hydrogen bonds. This designation implies that the covalent X–H bond lengthens slightly but remains intact in the complex. However, depending on the acidity of the proton donor and the basicity of the proton acceptor, partial proton transfer can occur to form complexes with *proton-shared* hydrogen bonds which have long X–H and Y–H distances relative to covalent bondlengths, but shorter X–Y distances. If further proton transfer occurs, the resulting complex becomes a hydrogen-bonded ion pair, the Y–H distance approaches the Y–H distance in the monomer cation, the X–H distance becomes much longer than the covalent X–H distance, and the X–Y distance lengthens slightly. Although ion-pair hydrogen-bonded complexes are not common in the gas-phase, a few have been characterized both experimentally and theoretically. The complex formed from HCl and $N(CH_3)_3$ has a proton-shared hydrogen bond, while HBr:$N(CH_3)_3$ has an ion-pair hydrogen bond [22]. These complexes are illustrated in Scheme 8. Structural characteristics of the different hydrogen-bond types can be seen from the X–H, N–H, and X–N distances in Table 1 for complexes of the hydrogen halides with NH_3 and $N(CH_3)_3$. The changes in hydrogen-bond type from normal to proton-shared to ion pair are smooth and continuous, and dependent on the degree of proton transfer. The degree of proton transfer can be enhanced by solvent and temperature effects, and mimicked theoretically by electric fields of varying strengths imposed along the hydrogen-bonding direction [23–27]. These effects will be discussed in more detail in the section on the vibrational spectra of hydrogen-bonded complexes.

Symmetric or asymmetric *proton-shared* hydrogen bonds may also be found in some protonated complexes. Scheme 9 illustrates the structure of the protonated water dimer $O_2H_5^+$ which has C_2 symmetry and a symmetric O···H···O hydrogen bond [28,29]. The dissociation energy D_e to $H_3O^+ + H_2O$ is 143 kJ mol^{-1}. The hydrogen-bonded O–H distances are longer (1.194 Å) than the O–H distances in the isolated hydronium ion OH_3^+ (0.980 Å) and water monomer (0.963 Å). The O–O distance is short (2.385 Å) compared to the O–O distance in the water dimer (2.98 Å). The central proton

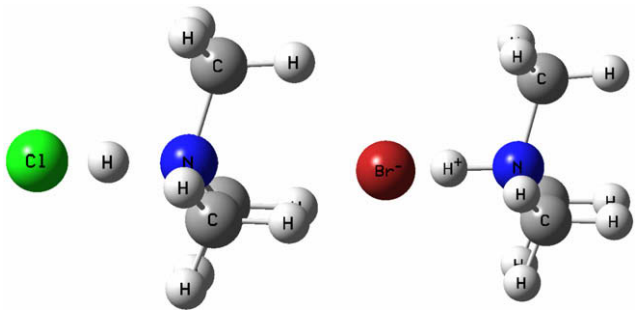

Scheme 8. The complexes of HCl and HBr with $N(CH_3)_3$.

Table 1
X–H, N–H, and X–N distances (R/Å) for complexes of hydrogen halides with NH_3 and $N(CH_3)_3$[a,b]

	Monomer	$FH:NH_3(T)$	$FH:N(CH_3)_3(T)$
R(F–H)	0.927	0 963	0.988
R(N–H)[c]		1.674	1.561
R(F–N)		2.637	2.549
	Monomer	$ClH:NH_3(T)$[d]	$ClH:N(CH_3)_3(PS)$[d]
R(Cl–H)	1.288	1.341	1.658
R(N–H)		1.739	1.167
R(Cl–N)		3.080	2.825 (2.816)[e]
	Monomer	$BrH:NH_3(T)$[d]	$BrH:N(CH_3)_3(IP)$[d]
R(Br–H)	1.407	1.462	1.870
R(N–H)[c]		1.785	1.113
R(Br–N)		3.247 (3.255)[e]	2.983 (2.96)[e]

[a] Hydrogen bond type given in parentheses. T = normal (traditional); PS = proton-shared; IP = ion-pair.
[b] Computed MP2/6-31+G(d,p) and MP2/aug′-cc-pVDZ data [23–25]. Data for $FH:N(CH_3)_3$ are MP2/6-31+G(d,p) results.
[c] The N–H distances in NH_4^+ and $^+HN(CH_3)_3$ are between 1.02 and 1.03 Å.
[d] Hydrogen-bond descriptions given by Legon [22].
[e] Experimental distances from Ref. [22].

Table 2
Computed and experimental frequency shifts ($\delta\nu$/cm^{-1}) of the X–H stretching band in complexes with *normal* X–H···Y hydrogen bonds[a]

Complex		Computed $\delta\nu$ (cm^{-1})	Experimental $\delta\nu$[b](cm^{-1})
FH···NCH		−262	−245 (v)
$FH···NCCH_3$		−343	−334 (v)
ClH···NCH		−113	−79 (v)
$ClH···NCCH_3$		−167	−155 (v)
FH···CO		−134	−117 (v)
$ClH···OH_2$		−177	−207 (v)
FH···FH		−116	−93 (v)
ClH···ClH		−32	−53 (Ar)
$HOH···OH_2$		−79	−64 (Ar)
$FH:CHCl_3$	Open	−65[c]	−78 (Ar)[d]
	Cyclic	−50[c]	−32 (Ar)[d]
$FH:CH_2Cl_2$	Bifurcated	−20[c]	−19 (Ar)[d]
	Cyclic	−111[c]	−120 (Ar)[d]

[a] Experimental and theoretical shifts reported in Ref. [32]. The computed values are from MP2/6-31+G(d,p) calculations.
[b] v = vapor; Ar = low-temperature Ar matrix.
[c] Ref. [15].
[d] Ref. [33].

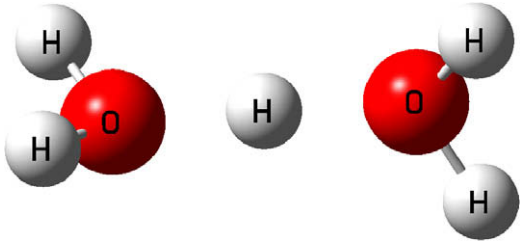

Scheme 9. The protonated water dimer $O_2H_5^+$.

in $O_2H_5^+$ can be thought of as forming an incipient hydronium ion with the two H_2O molecules and, like $[F–H–F]^-$, should perhaps be considered a chemically bound species rather than a hydrogen-bonded one.

3. Vibrational spectra of hydrogen-bonded complexes

Formation of a hydrogen-bonded complex from two nonlinear molecules converts three degrees of rotational and three degrees of translational freedom into six new low-frequency intermolecular modes with vibrational frequencies which usually lie below 400 cm^{-1}. In a typical complex, the intramolecular modes of the two hydrogen-bonded monomers are only slightly perturbed, an exception being the X–H stretching mode. This vibration characteristically shifts to lower frequency (a red shift) and greatly increases in intensity in the infrared (IR), though not in the Raman spectrum, upon formation of the X–H···Y hydrogen bond. The shift to lower frequency has generally been interpreted in terms of a lengthening and weakening of the X–H bond and the enhanced IR intensity to intermolecular polarization. For a series of complexes with the same proton donor, the magnitude of the shift can be related to the binding energy of the complex [30]. The red shift of the X–H stretching band and the large increase in IR intensity of this band have traditionally been recognized as the infrared spectroscopic signature of the hydrogen bond [5].

Ab initio calculations carried out with an appropriate wavefunction model and basis set [31], and using the harmonic approximation, can reasonably reproduce the shift of the X–H stretching band of complexes stabilized by *normal* hydrogen bonds. Table 2 provides a comparison of computed and experimental shifts for a set of complexes and shows fair agreement between them.

Under what circumstances does the harmonic approximation fail to provide a reliable estimate of the red shift of the X–H stretching frequency? The answer depends on the nature of the hydrogen bond and the nature of the potential surface. If the equilibrium structure is stabilized by a normal hydrogen bond and exists in a relatively deep potential energy well so that both the $v = 0$ and $v = 1$ vibrational states of the proton-stretching mode are confined within this well, then the harmonic approximation can reasonably estimate the shift of the X–H band. Such is the case for the complexes in Table 2. However, if in the $v = 0$ and/or $v = 1$ states of the proton-stretching mode the complex samples the proton-shared region of the surface, or if the complex is stabilized by a proton-shared hydrogen bond, then a parabola fails to describe the hydrogen-bonding region and a harmonic treatment of vibration is inadequate.

A set of complexes illustrating both the success and failure of the harmonic approximation are those with the hydrogen halides HX as proton donors to NH_3. These complexes have been shown experimentally and theoretically to have equilibrium structures stabilized by normal X–H···N hydrogen bonds [22,34,35]. The computed and experimental Ar-matrix spectra of the $FH:NH_3$ complex are shown in Fig. 1. The computed frequency of the F–H stretch is an underestimate because of the anharmonicity of the F–H stretch in the monomer and the influence of the matrix. Nevertheless, the computed and experimental spectra are similar, with the strongest band in each belonging to the proton-stretching vibration and appearing in the same spectral region, with the band in each spectrum similarly red-shifted relative to the isolated monomer.

However, the harmonic approximation breaks down for the $BrH:NH_3$ complex. Thus, the computed harmonic Br–H stretching frequency is 2006 cm^{-1} while the experimental value is 729 cm^{-1} [36,23]. This discrepancy arises primarily from the flatness of the potential surface surrounding the global minimum, and the accessibility of the proton-shared region of the surface in the $v = 1$ vibrational state, and to a lesser extent in the $v = 0$ state, of the proton-stretching mode. For this complex, a two-dimensional treatment of vibration which couples the proton- and dimer-stretching modes reduces the Br–H stretching frequency to 888 cm^{-1}, in much better agreement with experiment but still higher than the experimental frequency. The difference of 159 cm^{-1} has been attributed to the effect of the Ar matrix [23,24].

There are four strong bands between 1050 and 1450 cm^{-1} in the IR spectrum of $ClH:NH_3$ in an Ar matrix. The band at 1371 cm^{-1} has been assigned by Barnes et al. to the proton-stretching vibration

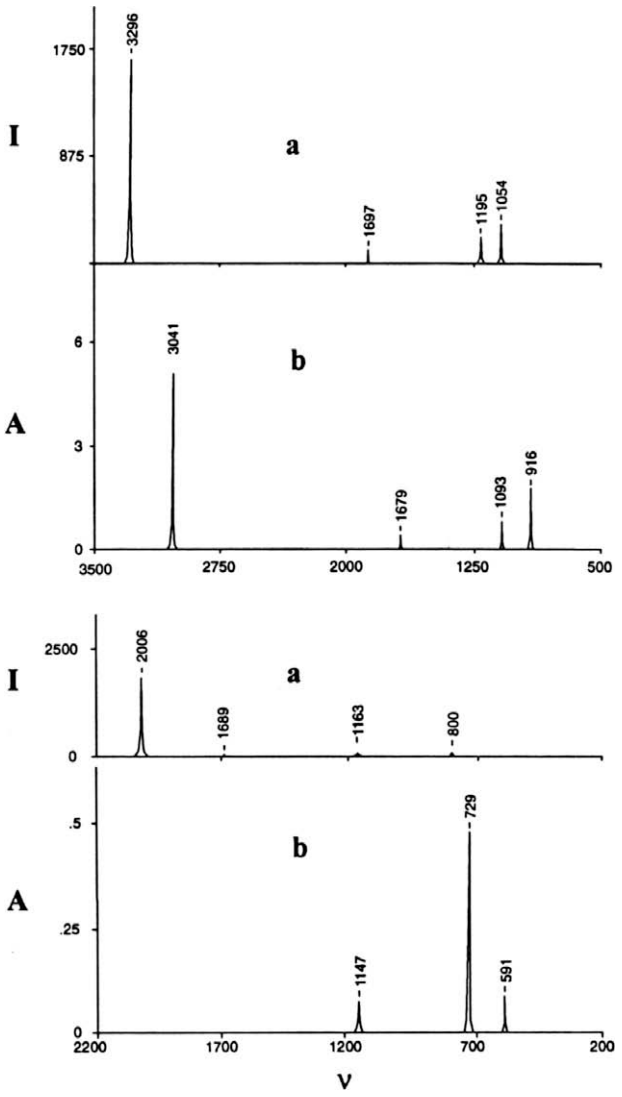

Fig. 1. Top pair $FH{:}NH_3$; bottom pair $BrH{:}NH_3$. For each pair the top spectrum is the computed gas-phase harmonic spectrum with intensity plotted against frequency. The bottom spectrum is the experimental spectrum in an Ar matrix, with absorbance plotted against frequency. In each case, the strongest band is the proton-stretching band (figure taken from Ref. [32]).

[37]. The computed harmonic Cl–H stretching frequency in $ClH{:}NH_3$ is 2289 cm^{-1}, much higher than the experimental value. A two-dimensional anharmonic treatment of vibration which couples the proton- and dimer-stretching modes reduces the stretching frequency to 1566 cm^{-1} [24]. Although the $v = 0$ vibrational state of the $ClH{:}NH_3$ complex is confined within the potential well surrounding the equilibrium structure, the $v = 1$ vibrational state samples the proton-shared region of the surface, and is responsible for the large correction. Multiple strong bands are found in the experimental spectrum in the region of the proton-stretching vibration for this complex. These arise from coupling of the proton-stretching vibration with vibrations of NH_3.

The harmonic approximation also breaks down for complexes stabilized by proton-shared hydrogen bonds. The flatness of the potential surface in the hydrogen-bonding region leads to large-amplitude motion by the proton, a situation which cannot be adequately described by a parabola. One example is the protonated water dimer $O_2H_5^+$ (Scheme 9) which has a symmetric O···H···O hydrogen bond. Ojamäe et al. computed the harmonic and anharmonic spectra for this complex [38]. The harmonic proton-stretching frequency is 983 cm^{-1} while the one- and two-dimensional anharmonic proton-stretching frequencies are higher at 1623 and 1275 cm^{-1}, respectively. The experimental gas-phase proton-stretching frequency is 1085 cm^{-1} [39]. In a study of O···H···O hydrogen bonds, Roscioli et al. [40] noted that the failure of their calculated *ab initio* harmonic spectra to recover the experimental bands provides evidence that the proton motions are indeed significantly anharmonic.

The agreement of the experimental and computed harmonic frequency for the $ClH{:}N(CH_3)_3$ complex with a proton-shared hydrogen bond must be considered fortuitous. The computed harmonic spectrum of $ClH{:}N(CH_3)_3$ exhibits three strong low-frequency bands at 1588, 1383 and 1184 cm^{-1} [24]. All of these involve the Cl–H stretch coupled to CH_3 vibrational modes. The strongest band in the experimental Ar-matrix spectrum occurs at 1486 cm^{-1} and has been assigned to the proton-stretching vibration by Barnes and Wright [41]; this band shifts to 1615 cm^{-1} in a N_2 matrix. Thus, the computed harmonic spectrum is fortuitously consistent with both the Ar and N_2 matrix spectra. The computed two-dimensional anharmonic gas-phase frequency for this complex is 1134 cm^{-1}. It is possible to simulate the effect of the matrix by applying electric fields of varying strengths along the hydrogen-bonding direction [23,42]. These fields stabilize the more polar hydrogen-bonded structures, and therefore facilitate proton transfer across the hydrogen bond. The two-dimensional anharmonic frequency increases to 1478 cm^{-1} when a weak field of 0.0040 a.u. is imposed, thereby mimicking the effect of the Ar matrix. A higher field further increases the proton-stretching frequency and brings it into agreement with the N_2 matrix value [24].

Deuteration of the proton donor has a major effect on the vibrational properties of a hydrogen-bonded complex. In the harmonic approximation, the ratio of stretching frequencies $\nu(D)/\nu(H)$ is 0.71, but this ratio is not found for $ClH{:}NH_3$ and $ClH{:}N(CH_3)_3$ and their deuterated isotopomers. Thus, the ratio $\nu(D)/\nu(H)$ determined experimentally for $ClD{:}ND_3/ClH{:}NH_3$ is 0.81 and 0.76 in Ar and N_2, respectively [42]. The experimental ratio for $ClD{:}N(CH_3)_3/ClH{:}N(CH_3)_3$ is 0.84 in Ar and 0.83 in N_2 [43]. The increase in the ratio is likely to be due to the lowering of the energy of the $v = 1$ state of the Cl–H stretch caused by its greater exposure to the proton-shared region of the potential surface.

4. Blue-shifting hydrogen bonds

Although the IR spectroscopic signature of the hydrogen bond is widely acknowledged to be the red shift of the X–H stretching band accompanied by an increase in intensity of this band, opposite spectroscopic features are observed in the so called *blue-shifting* hydrogen bond [44–46]. In such a bond a shortening of the X–H bond usually occurs.

Experimental studies of hydrogen bonds involving fluoroform have found blue shifts of the C–H stretching band and a reduction in its infrared intensity relative to that in the monomer [46–52]. For example, the C–H stretch in $F_3CH{\cdots}O(CH_3)_2$ dissolved in liquid Ar has a blue shift of 17 cm^{-1} [51]. Moreover, matrix-isolation experiments found that the metastable hydrogen-containing inert-gas molecules HRgX, where X is an atom or group of atoms with a high electron affinity and Rg an inert-gas atom, formed complexes such as $N_2{\cdots}HArF$, $N_2{\cdots}HKrF$ and $N_2{\cdots}HKrCl$ which exhibited large blue shifts of the H–Rg stretching mode [53,54]. Although many theoretical papers have addressed the blue-shift phenomenon [55–65], we enquire whether or not a single theory can explain both red- or blue-shifting X–H stretches and expansion or contraction of the X–H bondlength upon hydrogen-bond formation.

A perturbative theory of vibrational frequency shifts originally proposed to account for solvent effects in vibrational spectroscopy [66–68] has been found useful in predicting the direction of the frequency shift observed for hydrogen-bonded complexes. Excellent agreement with the standard variational *ab initio* supermolecule approach is obtained [51,64,65]. In this approach perturbation theory is used to determine the shift and X–H bondlength change due to the intermolecular potential energy U which is expanded as a power series in the displacement from equilibrium of the X–H bond, $U = U_e + U'\xi + \frac{1}{2}U''\xi^2 + \ldots$, where $\xi = (r - r_e)/r_e$; $U - U_e$ and the cubic anharmonicity are treated as perturbations to the X–H harmonic oscillator.

The complexation-induced wavenumber shift $\Delta\omega$ of the fundamental absorption band of a perturbed diatomic oscillator is related to U' and U'' via the equation [66]

$$Hc\Delta\omega = (B_e/\omega_e)(U'' - 3aU') \quad (1)$$

where $c\omega_e$ is the frequency of the harmonic oscillator, a the dimensionless cubic anharmonicity constant of the X–H oscillator, B_e its rotational constant $h/(8\pi^2 mcr_e^2)$ and m its reduced mass. The constants B_e, ω_e and a can be readily determined by *ab initio* computations while U' and U'' can be obtained numerically from three *ab initio* single-point energy computations on the interacting species. This expression can be extended to molecules larger than diatomics [68]. Eq. (1) shows that the magnitude and sign of the frequency shift are determined by the relative magnitude and signs of U' and U''. The first term in (1) arises from the change in the harmonic force constant due to the intermolecular interaction, and the second from a change in the equilibrium bond length r_e of the proton donor X–H bond. The second term is proportional to the bond-stretching force $-U'$, and the bondlength change of the oscillator Δr is [67]

$$\Delta r = -2B_e r_e U'/(hc\omega_e^2) \quad (2)$$

Eqs. (1) and (2) taken together imply that the shift $\Delta\omega$ and bondlength change Δr are not necessarily correlated in the usual red shift/bond extension and blue shift/bond contraction paradigm.

A theoretical study of linear dimers with Cl–H as the proton donor and N_2, CO and BF as proton acceptors illustrates the violation of this paradigm [64]. The perturbation model as well as standard *ab initio* supermolecule calculations at MP2 and QCISD have shown that a red shift of the H–Cl stretch and an elongation of the H–Cl bond occur if both U' and U'' are negative (FB···HCl and OC···HCl), while a blue shift and bond contraction are obtained if both U' and U'' are positive (BF···HCl). If U' is negative U'' may be negative or positive and the frequency change will depend on their relative magnitudes, giving a red shift and bond lengthening in N_2···HCl, which is not anomalous, but a blue shift and bond *lengthening* in CO···HCl [64].

The sign and magnitude of U' and U'' can be rationalized by considering the inert-gas complexes in Table 3. It is useful to employ the concept of 'hardness' as it relates to the proton-acceptor atom Y. Chemical hardness η indicates an atom's resistance to deformation of its electron density and is defined as the second derivative of the electronic energy E with respect to the number of electrons N under a constant bare-nuclear potential V [69],

$$\eta = (\partial^2 E/\partial N^2)_V \approx (I - A)/2 \quad (3)$$

where I and A are the ionization energy and electron affinity of the atom. The hardness of the inert-gas atoms decreases in the order Ne > Ar > Kr.

Hardness influences the size of the dipole induced in the inert-gas atom by X–H, an interaction that increases the attractive energy, so decreasing hardness correlates with an increasing attractive force on the proton donor. Increasing hardness implies an increasing repulsive interaction since the electrons are less easily deformed by the electric field of X–H. Table 3 shows that, for a given X–H, as the hardness of the atom decreases, a positive U' (ClH···Ne, NCH···Ne) or a small negative U' (FH···Ne, CNH···Ne) becomes a larger negative U'. The trend for U'' is even more striking. For all X–H, U'' is positive for interactions with Ne and becomes a large negative U'' when Kr is the inert gas.

A similar trend is evident for the linear hydrogen bonds in complexes with HCl and HCN reported in Table 4. The atom of the proton donor that is hydrogen bonded increases in hardness in the order B < C < N < O < F. The attractive $-U'$ and $-U''$ terms in FB···HCl and FB···HCN lead to elongation of the Cl–H and C–H bonds and red shifts of the corresponding stretching frequencies. However, with increasing hardness of the proton-acceptor atom, the X–H bond eventually contracts and the X–H stretching frequencies are blue-shifted in BF···HCl and BF···HCN. It is noteworthy that the proton-acceptor molecules in these complexes are isoelectronic and that the heteroatomic CO and BF acceptors behave quite differently depending on which end of the molecule is hydrogen bonded. It may be surprising that the fluorine end of BF is inferior to the boron end as a proton acceptor, but BF has a dipole moment of approximately 0.8 D in the direction B^-F^+, illustrating a limitation to the application of simple arguments based on electronegativity.

The reduction in IR C–H bond stretching intensity normally associated with blue-shifting hydrogen bonds involving F_3CH is a consequence of the negative derivative of its permanent dipole moment with respect to C–H bond elongation. The induced dipole can be considered to consist of two parts: the dipole induced in the proton acceptor by the electric field of F_3CH and the dipole induced in F_3CH by the field of the proton acceptor. The former has a negative derivative with respect to C–H bond elongation but the latter has a positive and dominant one because the derivative of the par-

Table 3
Complexation-induced properties of FH···Rg, ClH···Rg, NCH···Rg and CNH···Rg, for Rg = Ne, Ar, Kr[a]

Species	U_e (cm^{-1})	U' (cm^{-1})	U'' (cm^{-1})	Δr (Å)	$\Delta\omega$[b] (cm^{-1})	R(H···Y) (Å)
F–H···Ne	−201	−11.7	633	~0	+2.8 (+2.0)	2.2982
F–H···Ar	−220	−332	−1104	0.0007	−17.0 (−18.0)	2.5840
F–H···Kr	−292	−490	−1727	0.0011	−25.7 (−28.1)	2.7194
Cl–H···Ne	−158	88.7	1447	−0.0003	+7.4 (+7.1)	2.5143
Cl–H···Ar	−171	−92.2	−47.9	0.0003	−2.5 (−2.6)	2.8123
Cl–H···Kr	−255	−261	−870	0.0008	−9.8 (−9.9)	2.8757
NC–H···Ne	−187	69.1	778	−0.0002	+5.5 (+4.8)	2.5435
NC–H···Ar	−165	−21.1	87.1	0.0001	−0.2 (−0.6)	2.9275
NC–H···Kr	−226	−71.6	−361	0.0002	−3.6 (−4.1)	3.0131
CN–H···Ne	−211	−26.3	73.5	0.0001	−0.4 (−0.9)	2.3316
CN–H···Ar	−227	−278	−1930	0.0007	−17.3 (−17.4)	2.6527
CN–H···Kr	−312	−457	−2780	0.0011	−26.6 (−26.8)	2.7668

[a] MP2/6-311++G(2d,2p) values.
[b] *Ab initio* computed shifts are given in parenthesis.

Table 4
Complexation-induced properties of Y···HCl and Y···HCN[a]

Species	U_e (cm^{-1})	U' (cm^{-1})	U'' (cm^{-1})	Δr (Å)	$\Delta\omega$ (cm^{-1})
FB···HCl	−1110	−2409	−12240	0.0071	−102
OC···HCl	−750	−945	−3300	0.0028	−34.8
N_2···HCl	−590	−333	804	0.0010	−5.4
CO···HCl	−486	−137	1977	0.0004	3.6
BF···HCl	−286	133	2139	−0.0004	10.8
FB···HCN	−9543	−1707	−6778	0.0048	−78.0
OC···HCN	−15583	−897	−2748	0.0025	−37.2
N_2···HCN	−19985	−417	−754	0.0012	−14.9
CO···HCN	−15215	−150	377	0.0004	−2.4
BF···HCN	−8645	27	808	−0.0001	4.4

[a] The calculations on Y···HCl were carried out at the QCISD/6-311++G(3df,3pd) level; those for Y···HCN are at MP2/6-311++G(2d,2p).

allel component of the polarizability of F_3CH is large and positive. Since the IR intensity of the complex is proportional to the square of the derivative of the total dipole moment, it is reduced in these complexes. However, the IR intensity for some blue-shifted complexes, such as those with Cl–H as the proton donor to N_2, CO and BF, does increase upon complexation [64].

This analysis by the perturbation model makes it clear that red-shifting and blue-shifting hydrogen bonds can be described by the same theory. The latter should not therefore be considered to be fundamentally different.

5. Water

The remarkable properties of liquid and solid water are a consequence of the versatility of a single water molecule which can form two hydrogen bonds as a proton donor and two further hydrogen bonds as a proton acceptor. This ability is responsible for the abnormally high boiling point, which is 160 °C higher than that of H_2S, and for the tetrahedral coordination of each water molecule in normal ice, a structure that tends to persist in the liquid. The water dimer has 20 electrons and is therefore susceptible to highly accurate quantum-chemical computations, but definitive simulations of the properties of liquid water still present a significant challenge, despite the large number of studies devoted to this all-important ubiquitous substance. Many attempts have been made to understand the anomalous properties of water, such as its contraction on melting and further contraction on warming to 4 °C in H_2O and 11 °C in D_2O. The abnormalities are due to the competition between the preference for a water molecule to form four hydrogen bonds versus the requirement for efficient packing in the condensed phases, thereby reducing the number of nearest neighbors from the close-packed 12 to 4. The competition is somewhat relieved by the flexibility introduced by melting and further warming, giving rise to the anomalous contractions. The relief is greater in H_2O than in D_2O because of the larger amplitude of the oscillations in H_2O.

The intermolecular potential energy surface for two rigid molecules has six degrees of freedom, giving rise to six intermolecular variables; the dimensionality increases to twelve if the effect of monomer vibrations on the interaction of two water molecules is taken into account. The trimer has twelve intermolecular degrees of freedom and 21 in all. It is clear that judicious approximations will be needed for a rigorous theory of water.

The simplest water cluster is the hydrogen-bonded dimer. The microwave spectrum of the dimer yielded the structure of C_s symmetry in Scheme 1 with an O–O distance of 2.98 Å, and a nearly linear O–H···O hydrogen bond [12]. The dissociation energy D_e is 21 kJ mol^{-1} (1800 cm^{-1}). There are two first-order saddle points that are of special interest on the potential energy surface [19]. One is a cyclic dimer of C_i symmetry which is the transition structure for the interchange of the roles of proton donor and proton acceptor with a barrier of 3 kJ mol^{-1}. The other is bifurcated of C_{2v} symmetry and is a transition structure for the interchange of the two H atoms of the proton-donor molecule with a barrier of 8 kJ mol^{-1}. These two structures are illustrated in Scheme 10. Tunnelling motion of the protons (or deuterons in the case of $(D_2O)_2$) leads to energy-level splittings that provide the source of much quantitative information about the potential energy surface away from equilibrium [70,71]. The barrier height for the switching of protons of the acceptor OH_2 by rotation about the C_2 axis is ~2 kJ mol^{-1} [72].

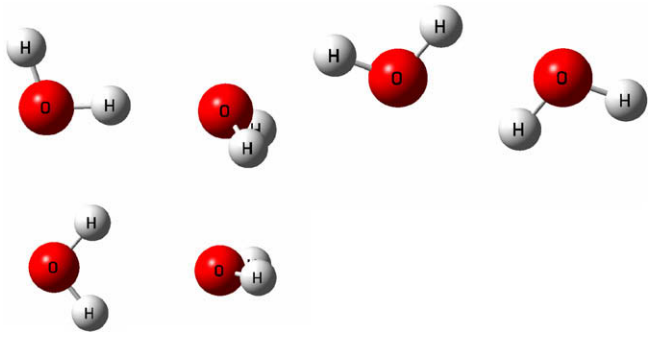

Scheme 10. The equilibrium, cyclic and bifurcated water dimers. The cyclic and bifurcated structures are actually first-order saddle points and have energies of 3 and 8 kJ mol^{-1} above equilibrium [19].

The potential surface for three water molecules has been characterized in detail [74–76]. The global minimum on the surface corresponds to a cyclic structure, with a dissociation energy D_e = 78 kJ mol^{-1} relative to three water monomers. Although the equilibrium structure is about 20 kJ mol^{-1} more stable that an open trimer with an O–H···O–H···O–H chain of hydrogen bonds, the binding energy per hydrogen bond for the cyclic trimer is less than that for the open trimer. The cyclic trimer has C_1 symmetry and is therefore chiral, but rapid tunnelling motion of the protons prevents separation into enantiomers. There are two metastable structures on the trimer potential surface. One has a single water molecule acting as a double proton acceptor and the other a single water molecule acting as a double proton donor. The binding energies per hydrogen bond for these two trimers are less than the dimer binding energy.

The potential surfaces for four, five and six water molecules are quite complicated, having many local minima and transition structures [77–80]. The global minima on the tetramer and pentamer surfaces are cyclic. As the size of the ring increases, the hydrogen bond approaches linearity and the O–O distance decreases, providing direct evidence for cooperativity [73]. For the hexamer three-dimensional cage-type structures become energetically favorable. Such structures dominate as the size of the cluster increases [77–80]. The cyclic trimer, tetramer, pentamer and hexamer are illustrated in Scheme 11.

Detailed knowledge of the structure and properties of water clusters is important for testing approximate potential energy surfaces but does not provide an understanding of the liquid. The customary approach to simulations of liquids is to employ an empirical potential that has been adjusted to give agreement with selected observed properties. Such potentials have their uses because of their simplicity but are not accurate for small clusters or for a definitive description of the liquid. The ideal would be to calculate rapidly and accurately the electronic energy for each configuration of the N molecules in the simulation, as in the Car-Parrinello approach, but this is not yet possible. Density functional calculations can compute energies quickly but current functionals are not able to give an accurate intermolecular surface and fail to

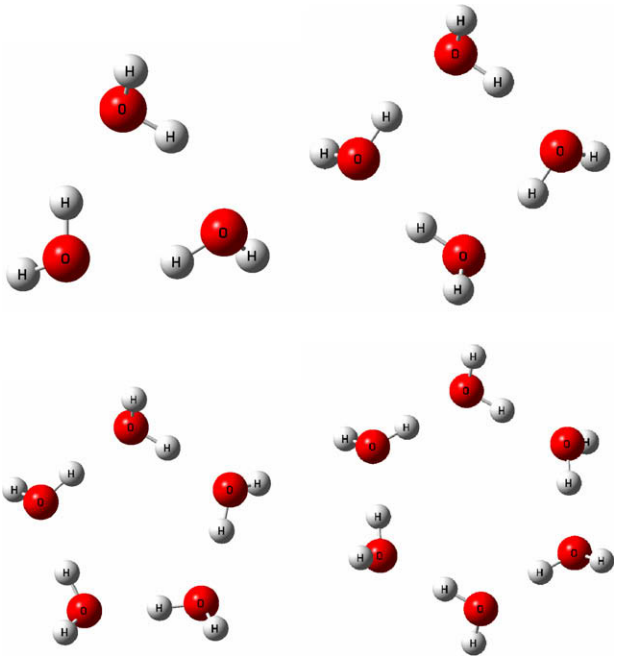

Scheme 11. The cyclic water trimer, tetramer, pentamer and hexamer.

account for the long-range electron correlation that gives rise to dispersion forces which are important contributors to the cohesive energy of all liquids.

The potential energy of a many-molecule cluster can be expressed as a sum of two-body, three-body, four-body, ... contributions. For practical purposes it is necessary to curtail the expansion at the three-body term and there is evidence that this can be a good approximation, although it has been suggested that the four-body term is important for the tetrahedral structure in water [81]. The most important many-body contribution to the interaction energy in dipolar liquids arises from the induction energy due to the distortion of the electron cloud by the strong electric fields of neighboring molecules [82]. It depends on the molecular polarizabilities that give the electric multipole moments induced by these fields; if the induced moments can be treated non-iteratively, this many-body contribution is limited to two- and three-body terms. The simplest description of induction involves the assignment of a single isotropic dipole polarizability to each molecule, leaving a choice for its location. There are other contributions to many-body molecular interactions, including dispersion energy, which is crucial in determining the nature of the close-packed structure of the inert-gas solids, and exchange repulsion, but in the case of water these are small.

There have been a number of important attempts to deduce a potential for gas-phase clusters and liquid water based on an accurate six-dimensional dimer surface together with an explicit use of tensorial polarizabilities [71,83–85]. Goldman et al. [71] use a semi-empirical anisotropic site potential [83] adjusted to describe terahertz vibration–rotation tunnelling spectroscopic data of high precision to deduce accurately properties of water clusters up to the hexamer and of liquid water, including the O–O, O–H and O–D radial distribution functions. The potential of Bukowski et al. [85] is deduced from *ab initio* CCSD(T) computations on 2510 selected grid points for a pair of rigid H_2O molecules. The computed energies were fitted to an analytic potential function which incorporated a single isotropic dipole polarizability near the O atom. The potential gives impressive agreement with spectroscopic data for the water dimer and with the radial distribution functions for the liquid. Recent work shows the need for using a potential that allows for monomer distortion; such distortion has been incorporated in an adiabatic model that allows the monomers to change their structure continuously with the position and orientation of a neighboring molecule [86].

Table 5 shows some properties of water and heavy water that challenge theory. A qualitative understanding emerges through consideration of the open structure maintained by the hydrogen bonds against the tendency for dense packing. It is interesting to note that the O–O distance in ice at 223 K is 2.759 Å and in liquid water it is 2.84 Å [73] despite the fact that ice is less dense than water; the tetrahedral rigidity enforced in ice by the hydrogen bonds is somewhat relaxed in the liquid, permitting the second, third, ... O–O neighbors to be closer packed in the liquid. The enhanced energy of the deuterium bond over the hydrogen bond, illustrated by the vaporization enthalpies in Table 5, is due to the two zero-point bending motions of the proton causing larger departures from the optimum linear bond. The H-bond stretching motion of a red-shifted hydrogen bond actually favors the H- over the D-bond since the shift is smaller for the latter and the zero-point stabilization is half the shift, but in most cases the bending motion is dominant [87]. Thus the dissociation energy D_0 of HF···DF is 1157 cm^{-1} and that of DF···HF is 1082 cm^{-1} [88]. OC···DCCH is preferred over OC···HCCD, and OC···H^{13}CCH over OC···HC^{13}CH by about 4:1 in a supersonic expansion because of the lesser zero-point departure from linearity [89,90]. The smaller molar volume of H_2O requires an explanation, since CH_4 in the condensed phase is bigger than CD_4 because the larger anharmonic zero-point vibrational motion increases the effective CH bondlength; the enhanced oscillatory intermolecular motion in H_2O apparently permits closer packing than in D_2O.

A test of the water dimer potential that is commonly applied is a comparison of the computed second virial coefficient [83,85], or the related Joule–Thomson coefficient [71], with experiment over a wide temperature range. A more critical comparison would be with the second dielectric virial coefficient which depends on the extra contribution to the dielectric constant of a gas of an interacting pair of molecules over that of two monomers [91]. Calculations show the sensitivity of this property to polarization and to the details of the short-range repulsive forces in the water dimer [92]. There is a need for new measurements of this under-exploited property.

6. Concluding remarks

Relative to chemical bonds, the hydrogen bond is weak, but in this weakness lies its importance. Because hydrogen bonds can easily be made and broken at ambient temperatures, they play a vi-

Table 5
Some properties of water and heavy water

	Temperature of maximum density (°C)	Molar volume at maximum density (cm^3/mol)	Melting point at 1 bar (°C)	Boiling point at 1 bar (°C)	Enthalpy of vaporization at 100 °C (kJ/mol)	Contraction on melting (cm^3/mol)	Viscosity at 20 °C (mPa s)
H_2O	3.984	18.011	0	100	40.0	1.63	1.005
D_2O	11.185	18.104	3.82	101.4	41.3	1.56	1.25

tal role in the chemistry of life. They are crucial in determining the tertiary structure of proteins and nucleic acids, the thermal properties of polymers such as nylon, and drug–receptor interactions. Hydrogen bonds can give rise to unusual properties, as in water. The fact that water remains liquid beneath ice and snow on lakes in winter may have been critical in the evolution of primitive life.

Advances in experiment and theory and in computing power provide a great opportunity for understanding and exploiting the special properties of hydrogen-bonded systems. Important progress has recently been made towards a fundamental description of water from first principles but much remains to be done, including incorporation of the effects of molecular vibrations and proton transfer. Is nonlinear polarization involving molecular hyperpolarizabilities significant? Does long-range correlation of proton fluctuations contribute a significant binding force in liquid water and ice analogous to that in the inert gases arising from long-range electron correlation? Large proton polarizabilities that arise from these fluctuations have been much studied by Zundel [93]. The importance of polarization, and its major contribution to many-body interactions, is now recognized and its role in determining organic crystal structures is the subject of a recent paper [94].

In this Letter we have presented our personal, and therefore restricted, view of the hydrogen bond, a topic with a tremendous variety of applications and consequences in many fields of science. We have neglected areas such as solvation and the hydrophobic effect, where entropic forces drive non-polar molecules together in aqueous solution with a force that *increases* with rising temperature [95]. We have not discussed the important effects of hydrogen bonding on NMR spectra, although there have been recent advances in understanding the increase in the proton nuclear magnetic shielding parallel to the H-bond and large decrease in the perpendicular component [96], and in nuclear spin–spin coupling across a hydrogen bond [97]. We can expect significant advances in our understanding of the nature of the hydrogen bond in the next decade, but the breadth of its influence means it will remain perpetually young.

References

[1] P.W. Atkins, J. de Paula, Atkins' Physical Chemistry, W.H. Freeman, San Francisco, eighth edn., 2006, p. 634.
[2] Current Science 92 (2007) 17.
[3] D.A. Smith, Modeling the Hydrogen Bond, in: D.A. Smith, ACS Symposium Series, vol. 569, 1994, p. 1.
[4] D. Hadži, Theoretical Treatments of Hydrogen Bonding, in: D. Hadži (Ed.), John Wiley & Sons, Chichester, 1997, p. xi.
[5] G.C. Pimentel, A.L. McClellan, The Hydrogen Bond, W.H. Freeman & Co., San Francisco, 1960.
[6] Theoretical Treatments of Hydrogen Bonding, D. Hadži (Ed.), John Wiley & Sons, Chichester, 1997.
[7] S. Scheiner, Hydrogen Bonding. A Theoretical Perspective, Oxford University Press, 1997.
[8] G.A. Jeffrey, An Introduction to Hydrogen Bonding, Oxford University Press, 1997.
[9] G.R. Desiraju, T. Steiner, The Weak Hydrogen Bond, Oxford University Press, 1999.
[10] C.A. Coulson, Research 10 (1957) 159.
[11] T. Dyke, B.J. Howard, W. Klemperer, J. Chem. Phys. 56 (1969) 2442.
[12] T. Dyke, J.S. Muenter, J. Chem. Phys. 60 (1974) 2929.
[13] M.W. Feyereisen, D. Feller, D.A. Dixon, J. Phys. Chem. 100 (1996) 2993.
[14] D.R. Hunt, L. Andrews, J. Phys. Chem. 96 (1992) 6945.
[15] J.E. Del Bene, H.D. Mettee, J. Phys. Chem. 97 (1993) 9650.
[16] A. Held, D.W. Pratt, J. Am. Chem. Soc. 115 (1993) 9708.
[17] J.E. Del Bene, J. Phys. Chem. 98 (1994) 5902.
[18] G.M. Florio, C.J. Gruenloh, T.S. Zwier, J. Chem. Phys. 113 (2000) 11143.
[19] G.S. Tschumper, M.L. Leininger, B.C. Hoffman, E.F. Valeev, H.F. Schaefer III, M. Quack, J. Chem. Phys. 116 (2002) 690.
[20] A.J. Gotch, T.S. Zwier, J. Chem. Phys. 96 (1992) 3388.
[21] H.S. Gutowski, T. Emilsson, E. Arunan, J. Chem. Phys. 99 (1993) 4883.
[22] A.C. Legon, Chem. Soc. Rev. 22 (1993) 153.
[23] J.E. Del Bene, M.J.T. Jordan, P.M.W. Gill, A.D. Buckingham, Mol. Phys. 92 (1997) 429.
[24] J.E. Del Bene, M.J.T. Jordan, Chem. Phys. 108 (1998) 3205.
[25] M.J.T. Jordan, J.E. Del Bene, J. Am. Chem. Soc. 122 (2000) 2101.
[26] N.S. Golubev, I.G. Shenderovich, S.N. Smirnov, G.S. Denisov, H.-H. Limbach, Chem. Eur. J. 5 (1999) 492.
[27] I.G. Shenderovich, A.P. Burtsev, G.S. Denisov, N.S. Golubev, H.-H. Limbach, Magn. Reson. Chem. 39 (2001) S91.
[28] L. Ojamäe, I. Shavitt, S.J. Singer, J. Chem. Phys. 109 (1998) 5547.
[29] X. Huang, B.J. Braams, J.M. Bowman, J. Chem. Phys. 122 (2005) 44308.
[30] J.E. Del Bene, W.B. Person, K. Szczepaniak, Mol. Phys. 89 (1996) 47.
[31] J.E. Del Bene, I. Shavitt, in: S. Scheiner (Ed.), Molecular Interactions: From Van der Waals to Strongly Bound Complexes, John Wiley and Sons, Inc., Sussex, 1997, p. 157.
[32] J.E. Del Bene, M.J.T. Jordan, Int. Rev. Phys. Chem. 18 (1999) 119.
[33] R.D. Hunt, L. Andrews, J. Phys. Chem. 96 (1992) 6945.
[34] N.W. Howard, A.C. Legon, J. Chem. Phys. 86 (1987) 6722.
[35] J.E. Del Bene, M.J.T. Jordan, Theochem 573 (2001) 11.
[36] W.B. Person, K. Szczepaniak, 1997, private communication.
[37] A.J. Barnes, T.R. Beech, Z. Mielke, J. Chem. Soc. Faraday Trans. II 80 (1984) 455.
[38] L. Ojamäe, I. Shavitt, J. Singer, Int. J. Quant. Chem. Quant. Chem. Symp. 29 (1995) 657.
[39] J.M. Headrick, E.G. Diken, R.S. Walters, N.I. Hammer, R.A. Christie, J. Cui, V.M. Myshakin, M.A. Duncan, M.A. Johnson, K.D. Jordan, Science 308 (2005) 1765.
[40] J.R. Roscioli, L.R. McCunn, M.A. Johnson, Science 316 (2007) 249.
[41] A.J. Barnes, M.P.J. Wright, Chem. Soc. Faraday Trans. 2 82 (1986) 153.
[42] J. Bevitt, K. Chapman, D. Crittenden, M.J.T. Jordan, J.E. Del Bene, J. Phys. Chem. A 105 (2001) 3371.
[43] A.J. Barnes, N.S. Kuzniarski, Z. Mielke, Chem. Soc. Faraday Trans. II 80 (1984) 465.
[44] P. Hobza, Z. Havlas, Chem. Rev. 100 (2000) 4253. and references contained therein.
[45] P. Hobza, Z. Havlas, Theor. Chem. Acc. 108 (2002) 325.
[46] A.J. Barnes, J. Mol. Struct. 704 (2004) 3.
[47] G.T. Trudeau, J.-M. Dumas, P. Dupuis, M. Guerin, C. Sandorfy, Top. Curr. Chem. 93 (1980) 91.
[48] M. Budesinsky, P. Fiedler, Z. Arnold, Synthesis (1989) 858.
[49] I.E. Boldeskul, I.F. Tsymbal, E.V. Ryltsev, Z. Latajka, A.J. Barnes, J. Mol. Struct. 436 (1997) 167.
[50] W. Caminati, S. Melandri, P. Moreschini, P.G. Favero, Angew. Chem., Int. Ed. Engl. 38 (1999) 2924.
[51] B.J. van der Veken, W.A. Herrebout, R. Szostak, D.N. Shchepkin, Z. Havlas, P. Hobza, J. Am. Chem. Soc. 123 (2001) 12290.
[52] P. Hobza, V. Spirko, Z. Havlas, K. Buchhold, B. Reimann, H.-D. Barth, B. Brutschy, Chem. Phys. Lett. 299 (1999) 180.
[53] A. Lignell, L. Khriachtchev, M. Pettersson, M. Rasanen, J. Chem. Phys. 117 (2002) 961.
[54] A. Lignell, L. Khriachtchev, M. Pettersson, M. Rasanen, J. Chem. Phys. 118 (2003) 11120.
[55] Y.L. Gu, T. Kar, S. Scheiner, J. Am. Chem. Soc. 121 (1999) 9411.
[56] S. Scheiner, T. Kar, J. Phys. Chem. A 106 (2002) 1784.
[57] W.A. Herrebout, S.N. Delanoye, B.J. Van der Veken, J. Phys. Chem. A 108 (2004) 6059.
[58] K. Hermansson, J. Phys. Chem. 106 (2002) 4695.
[59] X. Li, L. Liu, H.B. Schlegel, J. Am. Chem. Soc. 124 (2002) 9639.
[60] I.V. Alabugin, M. Manoharan, S. Peabody, F. Weinhold, J. Am. Chem. Soc. 125 (2003) 5973.
[61] S.A.C. McDowell, Phys. Chem. Chem. Phys. 5 (2003) 808.
[62] S.A.C. McDowell, Curr. Org. Chem. 10 (2006) 791. and references cited therein.
[63] A. Karpfen, J. Mol. Struct. (THEOCHEM) 710 (2004) 85.
[64] S.A.C. McDowell, A.D. Buckingham, J. Am. Chem. Soc. 127 (2005) 15515.
[65] S.A.C. McDowell, A.D. Buckingham, Spectrochim. Acta Part A 61 (2005) 1603.
[66] A.D. Buckingham, Proc. Roy. Soc. London Ser. A 248 (1958) 169.
[67] A.D. Buckingham, Proc. Roy. Soc. London Ser. A 255 (1960) 32.
[68] A.D. Buckingham, Trans. Faraday Soc. 56 (1960) 753.
[69] R.G. Parr, R.G. Pearson, J. Am. Chem. Soc. 105 (1983) 7512.
[70] R.J. Saykally, G.A. Blake, Science 259 (1993) 1570.
[71] N. Goldman, C. Leforestier, R.J. Saykally, Philos. Trans. Roy. Soc. A 363 (2005) 493.
[72] R.S. Fellers, C. Leforestier, L.B. Braly, M.G. Brown, R.J. Saykally, Science 284 (1999) 945.
[73] K. Liu, J.D. Cruzan, R.J. Saykally, Science 271 (1995) 929.
[74] D.J. Wales, J. Am. Chem. Soc. 115 (1993) 11180.
[75] O. Mó, M. Yáñez, J. Elguero, J. Chem. Phys. 97 (1992) 6628.
[76] F.N. Keutsch, R.J. Saykally, Proc. Nat. Acad. Sci. 98 (2001) 10533.
[77] A. Lenz, L. Ojamäe, J. Phys. Chem. A 110 (2006) 13388.
[78] S.Y. Fredericks, K.D. Jordan, T. Zwier, J. Phys. Chem. 100 (1996) 7810.
[79] S. Bulusu, S. Yoo, E. Aprà, S. Xantheas, X.C. Zeng, J. Phys. Chem. A 100 (2006) 11781.
[80] G.S. Fanourgakis, E. Aprà, S.S. Xantheas, J. Chem. Phys. 121 (2004) 2655.
[81] R. Bukowski, K. Szalewicz, G. Groenenboom, A. van der Avoird, J. Chem. Phys. 125 (2006) 44301.
[82] M.P. Hodges, A.J. Stone, S.S. Xantheas, J. Phys. Chem. A 101 (1997) 9163.
[83] C. Millot, J.C. Soetens, M.T.C. Martins Costa, M.P. Hodges, A.J. Stone, J. Phys. Chem. A 102 (1998) 754.
[84] E.M. Mas, R. Bukowski, K. Szalewicz, J. Chem. Phys. 118 (2003) 4404.
[85] R. Bukowski, K. Szalewicz, G. Groenenboom, A. van der Avoird, Science 315 (2007) 1249.
[86] Y. Scribano, N. Goldman, R.J. Saykally, C. Leforestier, J. Phys. Chem. A 110 (2006) 5411.

[87] A.D. Buckingham, Liu Fan-Chen, Int. Revs. Phys. Chem. 1 (1981) 253.
[88] L. Oudejans, R.E. Miller, J. Phys. Chem. A 101 (1997) 7582.
[89] A.C. Legon, A.L. Wallwork, J.W. Bevan, Z. Wang, Chem. Phys. Lett. 180 (1991) 57.
[90] S.A.C. McDowell, A.D. Buckingham, Chem. Phys. Lett. 180 (1991) 551.
[91] A.D. Buckingham, J.A. Pople, Trans. Faraday Soc. 51 (1955) 1179.
[92] A.J. Stone, Y. Tantirungrotechai, A.D. Buckingham, Phys. Chem. Chem. Phys. 2 (2000) 429.
[93] B. Brzezinski, G. Zundel, Faraday Discuss. 103 (1996) 363.
[94] G.W.A. Welch, P.G. Karamertzanis, A.J. Misquita, A.J. Stone, S.L. Price, J. Chem. Theory Comput. 4 (2008) 522.
[95] N.T. Skipper, C.H. Bridgeman, A.D. Buckingham, R.L. Mancera, Faraday Discuss. 103 (1996) 141.
[96] S.A.C. McDowell, A.D. Buckingham, Mol. Phys. 104 (2006) 2527.
[97] J.E. Del Bene, J. Elguero, in: J. Leszczynski (Ed.), Computational Chemistry, Reviews of Current Trends, vol. 10, World Scientific Publishing Co., Singapore, 2006, p. 229.

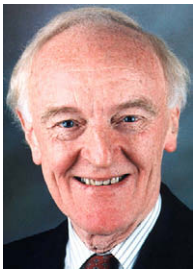

David Buckingham obtained a B.Sc. and M.Sc. from the University of Sydney in Australia. He was John Pople's first research student and received his Cambridge Ph.D. in 1956. He was a lecturer in Oxford from 1955 to 1965, professor at Bristol University from 1965 to 1969 and professor .at Cambridge from 1969 to 1997. He was editor of Chemical Physics Letters from 1978 to 1999. His research interests are in intermolecular forces and optical, electric and magnetic properties of molecules. He is a Fellow of the Royal Society, Corresponding Member of the Australian Academy of Science and a Foreign Associate of the National Academy of Sciences.

Janet Del Bene is Professor Emeritus of Chemistry at Youngstown State University (YSU). She received B.S. and B.A degrees from YSU, and her Ph.D. in 1968 from the University of Cincinnati (with Hans Jaffé). After postdoctoral fellowships at the Theoretical Chemistry Institute and Mellon Institute (with John Pople), she joined the faculty at YSU. Her primary research interests are in ab initio studies of hydrogen bonding, with emphasis on vibrational and magnetic properties. She is a Fellow of the American Association for the Advancement of Science and received the Morley Medal of the Cleveland Section of the American Chemical Society in 2008.

Sean McDowell received a BSc from the University of the West Indies (UWI) Mona Campus, Jamaica in 1985, and a PhD (with A.D. Buckingham) from Cambridge in 1992. After postdoctoral studies at the University of Western Ontario in Canada (1993–1996), he joined the staff of the UWI Cave Hill Campus, Barbados in 1997 where he is currently professor of theoretical chemistry. He is a member of the Royal Society of Chemistry and has received recognition from the Caribbean Academy of Sciences (Young Scientist Award, 1999) and from the UWI (Vice-Chancellor's Award for Excellence in Research, 2004).